ELSEVIER

www.elsevier.nl/locate/jorganchem

Journal of Organometallic Chemistry 611 (2000) 332–342

Journal of Organometallic Chemistry

Review

The chemistry of organo(silyl)platinum(II) complexes relevant to catalysis

Fumiyuki Ozawa *

Department of Applied Chemistry, Faculty of Engineering, Osaka City University, Sumiyoshi-ku, Osaka 558-8585, Japan

Received 14 March 2000; accepted 19 March 2000

Abstract

A variety of silylplatinum complexes *cis*- and *trans*-$PtR(SiYPh_2)L_2$ (R = Me, Et, Pr, Bu, vinyl, phenyl, phenylethynyl; Y = Ph, Me, H, F, OMe; L = $PMePh_2$, PMe_2Ph), *cis*-$Pt(SiR_3)(SnMe_3)(PMe_2Ph)_2$ (SiR_3 = $SiMe_3$, $SiMe_2Ph$, $SiMePh_2$, $SiPh_3$), and *cis*-$Pt(SiR_3)_2(PMe_2Ph)_2$ (SiR_3 = $SiMe_2Ph$, $SiMePh_2$, $SiPh_3$) have been prepared, and their structures and reactivities toward C–Si bond formation and phenylacetylene insertion have been examined by X-ray diffraction analysis, NMR spectroscopy, and kinetic experiments. Three types of processes are operative for C–Si bond formation from *cis*-$PtR(SiYPh_2)L_2$ complexes giving $RSiYPh_2$. One is the direct C–Si reductive elimination; most of the complexes follow this process. The second type involves isomerization of *cis*-$PtR(SiYPh_2)L_2$ to *cis*-$PtY(SiRPh_2)L_2$, followed by Y–Si reductive elimination; this process has been observed for *cis*-$PtR(SiPh_3)L_2$ (R = Et, Pr, Bu) and *cis*-$PtR(SiHPh_2)L_2$ (R = Me, Et, Pr, Bu). Reactions of alkyl–silyl complexes with hydrosilanes also afford the corresponding alkylsilanes quantitatively, constituting the third type of process. Insertion of phenylacetylene into the Pt–Si bond of $PtR(SiPh_3)L_2$ complexes takes place only for the *cis* isomers. Silyl–stannyl complexes undergo competitive insertion of phenylacetylene into the Pt–Si and Pt–Sn bonds under kinetic conditions, whereas the insertion into the Pt–Si bond predominates under thermodynamic conditions. Reactivities of four Pt–SiR_3 bonds toward insertion relative to the Pt–$SnMe_3$ bond have been evaluated: $SiMe_3$ (> 49) > $SiMe_2Ph$ (1.9) > $SiMePh_2$ (0.69) > $SiPh_3$ (0.075). Bis-silyl complexes exhibit a rather intricate dependence of the insertion reactivity upon the sorts of silyl ligands, not simply correlated with the reactivity of Pt–SiR_3 bonds, owing to the insertion process involving prior dissociation of a phosphine ligand. The bis-silyl complexes have a twisted square planar structure significantly distorted from planarity, and the rate of phosphine dissociation is highly sensitive to this distortion.

Keywords: Silyl complex; Platinum; X-ray structures; C–Si bond formation; Reductive elimination; Insertion; Kinetic study

1. Introduction

Catalytic addition of inter-element linkages to unsaturated hydrocarbons has attracted a great deal of recent interest [1,2]. The addition of a silicon–element bond catalyzed by a platinum-group metal complex is among the central subjects of such reactions. The classical examples include hydrosilylation and bis-silylation of alkenes and alkynes [3,4]. More recently, a variety of silicon–element bonds including Si–B [5,6], Si–Sn [7], and Si–S [8] have been applied to the catalysis, and the scope of applications has been remarkably expanded [1,2]. Organosilicon compounds thus prepared are important tools in organic synthesis. They also occur as building blocks in various synthetic materials [9].

Scheme 1 illustrates essential features of the catalytic cycle generally accepted. The first step is oxidative addition of a silicon–element bond (Si–E) to a low valent metal species **A**. Insertion of a C–C multiple bond into either the metal–silicon bond or the metal–element bond in **B** forms intermediate **C** or **D**, respectively. The subsequent C–E or C–Si reductive elimination gives the addition product with regeneration of **A**.

Among the elementary processes thus presumed, the oxidative addition has been relatively well documented,

* Fax: +81-6-605-2978.
E-mail address: ozawa@a-chem.eng.osaka-cu.ac.jp (F. Ozawa).

0022-328X/00/$ - see front matter
PII: S0022-328X(00)00493-9

especially for Si–H and Si–Si bonds [1,10]. On the other hand, little is known about the insertion and reductive elimination processes [11]. For example, although it has been reported that isolated bis(silyl)-palladium and -platinum complexes react with alkenes and alkynes to give bis-silylation products [12], direct observations of each elementary process (i.e. insertion into a M–Si bond and C–Si reductive elimination) have been extremely limited [13–15]. This is probably due to the instability of the alkyl (or alkenyl) silyl intermediates, formed by the insertion of alkene or alkyne into bis-silyl complexes.

Table 1 summarizes bond dissociation energies between Group 14 elements and platinum or palladium, estimated by thermochemical and theoretical studies [16]. It is seen that metal–silicon bond is much stronger than the corresponding metal–carbon bond. Nevertheless, the reactivity of silyl metal complexes, inferred from catalytic and stoichiometric silylation reactions, is much higher than that of common organometallic complexes, especially for platinum systems. This fact indicates that the highly reactive nature of silyl complexes is mainly due to kinetic reasons. Therefore, we have been interested in the reaction chemistry of platinum silyl.

In this paper, we wish to summarize our recent studies on the structures and reactivities of silylplatinum complexes in two sections. The first section deals with C–Si bond formation from *cis*-PtR(SiYPh$_2$)L$_2$ type complexes [17–23]. The succeeding section describes insertion reactions of phenylacetylene into a platinum–silicon bond [24–27]. Proper choice of supporting ligands has rendered the starting and/or product organo(silyl)platinum complexes stable enough for isolation to permit clean kinetic experiments. This is the first mechanistic study on C–Si bond formation and insertion reactions into a metal–silicon bond using solution kinetics.

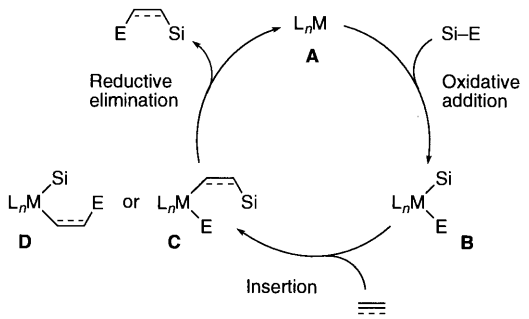

Scheme 1.

Table 1
Bond dissociation energies of M–E bonds in kcal mol^{-1}

System	Bond energy	Method	Reference
Pt–CH_3	32.3	Thermochemical	[16a]
Pt–$SiMe_3$	55.7		
Pt–$GeMe_3$	43.5		
Pt–$SnMe_3$	32.3		
Pd–CH_3	26.3	Theoretical	[16b]
Pd–SiH_3	44.5	(at CCSDT level)	
Pd–GeH_3	38.6		
Pd–SnH_3	37.5		
CH_3–CH_3	95.3	Theoretical	[16b]
CH_3–SiH_3	86.7	(at CCSDT level)	
CH_3–GeH_3	78.6		
CH_3–SnH_3	68.9		

2. C–Si bond formation

2.1. Stereoselective synthesis of cis and trans isomers

The *cis*- and *trans*-PtR(SiYPh$_2$)L$_2$ complexes prepared in this study are listed in Chart 1. Since it has been established that the reactivity of square planar, d^8 metal complexes toward reductive elimination is strongly affected by the configuration around metal center [28], we first examined stereoselective synthesis of the two geometrical isomers.

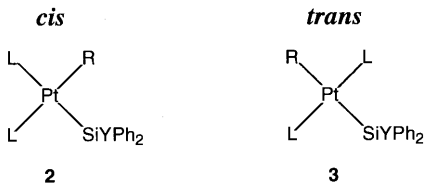

Chart 1.

Complex	R	SiYPh$_2$	L
2a	Me	$SiPh_3$	$PMePh_2$
2b	Me	$SiPh_3$	PMe_2Ph
2c	Et	$SiPh_3$	PMe_2Ph
2d	Pr	$SiPh_3$	PMe_2Ph
2e	Bu	$SiPh_3$	PMe_2Ph
2f	Bu	$SiMePh_2$	PMe_2Ph
2g	Bu	$SiFPh_2$	PMe_2Ph
2h	Bu	$Si(OMe)Ph_2$	PMe_2Ph
2i	Me	$SiHPh_2$	PMe_2Ph
2j	Et	$SiHPh_2$	PMe_2Ph
2k	Pr	$SiHPh_2$	PMe_2Ph
2l	Bu	$SiHPh_2$	PMe_2Ph
2m	$CH{=}CH_2$	$SiPh_3$	PMe_2Ph
2n	C≡CPh	$SiPh_3$	PMe_2Ph
2o	Ph	$SiPh_3$	PMe_2Ph
2p	Ph	$SiMePh_2$	PMe_2Ph
2q	Ph	$SiEtPh_2$	PMe_2Ph
2r	Ph	$SiPrPh_2$	PMe_2Ph
2s	Ph	$SiBuPh_2$	PMe_2Ph
3a	Me	$SiPh_3$	$PMePh_2$
3b	Me	$SiPh_3$	PMe_2Ph

3c	Et	$SiPh_3$	PMe_2Ph
3m	$CH{=}CH_2$	$SiPh_3$	PMe_2Ph
3n	$C{\equiv}CPh$	$SiPh_3$	PMe_2Ph
3o	Ph	$SiPh_3$	PMe_2Ph
3p	Ph	$SiMePh_2$	PMe_2Ph

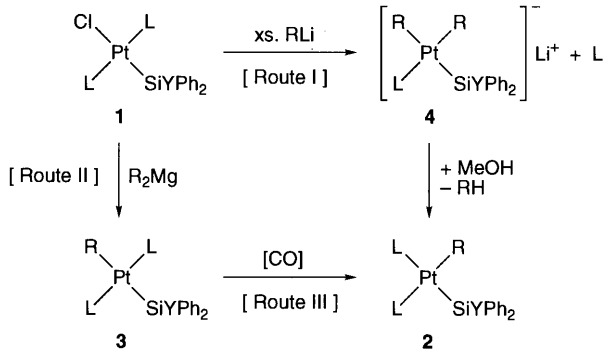

Scheme 2.

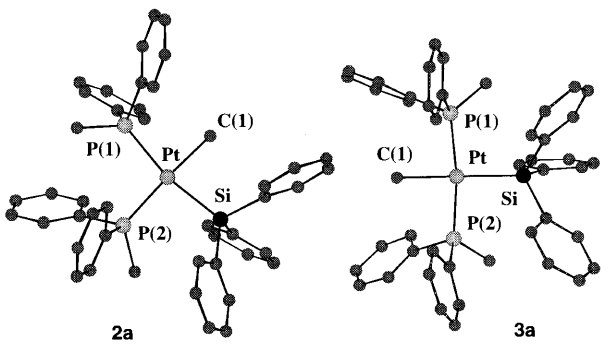

2a

Pt–C(1)	= 2.113(7) Å
Pt–Si	= 2.381(2) Å
Pt–P(1)	= 2.361(2) Å
Pt–P(2)	= 2.293(2) Å
C(1)–Pt–Si	= 82.2(2)°
P(1)–Pt–P(2)	= 98.02(7)°

3a

Pt–C(1)	= 2.16(2) Å
Pt–Si	= 2.412(6) Å
Pt–P(1)	= 2.275(6) Å
Pt–P(2)	= 2.283(6) Å
C(1)–Pt–Si	= 175.3(7)°
P(1)–Pt–P(2)	= 168.8(2)°

Fig. 1. CHEM-3D views of the X-ray structures of **2a** ($R = 0.038$) and **3a** ($R = 0.056$).

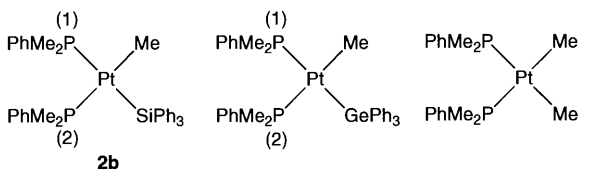

2b

P(1) δ –3.7 (d)	P(1) δ –4.6 (d)	δ –10.1 (s)
$^1J_{Pt-P}$ = 1330 Hz	$^1J_{Pt-P}$ = 1955 Hz	$^1J_{Pt-P}$ = 1844 Hz
$^2J_{P-P}$ = 19 Hz	$^2J_{P-P}$ = 19 Hz	
$^2J_{Si-P}$ = 198 Hz		
P(2) δ –10.9 (d)	P(2) δ –12.2 (d)	
$^1J_{Pt-P}$ = 2048 Hz	$^1J_{Pt-P}$ = 1972 Hz	
$^2J_{P-P}$ = 19 Hz	$^2J_{P-P}$ = 19 Hz	

Fig. 2. Comparison of ^{31}P-NMR data between **2b** and related complexes.

Scheme 2 summarizes the synthetic routes. The basis of stereocontrol is our previous studies on dialkylpalladium complexes [29]. The *cis* isomers of alkyl complexes (**2a**–**l**) were synthesized by using dialkyl(silyl)platinate intermediates **4**, generated in situ from *trans*-$PtCl(SiYPh_2)L_2$ (**1**) and excess amounts of alkyllithiums (Route I) [17,25]. Treatment of **4** with MeOH at low temperature led to selective protonation at the more electron-rich alkyl ligand, which is situated *trans* to the silyl ligand. Hence the *cis* isomers **2** were exclusively formed. On the other hand, since dialkylmagnesiums do not form the ate complexes owing to the less ionic nature [30], their reactions with **1** took place with retention of the *trans* configuration, giving the *trans* isomers **3a**–**c** in almost quantitative yields (Route II) [17,25].

Route I could not be applied to the *cis* isomers with vinyl, phenylethynyl, and phenyl ligands (**2m**–**p**). Thus the treatment of **1** with corresponding organolithiums followed by methanolysis provided a mixture of *trans* and *cis* isomers. Pure **2m**–**p** were prepared by isomerization of the *trans* isomers **3m**–**p** instead (Route III) [20–22]. Interestingly, carbon monoxide served as a good promoter for the isomerization, where no CO insertion into Pt–C bonds took place. On the other hand, *trans*-alkyl–silyl complexes **3a**–**c** readily underwent the insertion of CO to give *cis*-acyl(silyl)platinum complexes [25].

Fig. 1 shows X-ray structures of the *cis* and *trans* isomers of $PtMe(SiPh_3)(PMePh_2)_2$ (**2a** and **3a**) [17]. A notable structural feature arises from high *trans* influence of the silyl ligands, which leads to elongation of the M–E bonds *trans* to these ligands. For example, in the structure of **2a**, the Pt–P(1) bond (2.361(2) Å), *trans* to the $SiPh_3$ ligand, is about 0.07 Å longer than the Pt–P(2) bond (2.293(2) Å). It is also noted that the Pt–C(1) bond of **3a** (2.16(2) Å) is about 0.05 Å longer than that of **2a** (2.113(7) Å).

Fig. 2 compares the ^{31}P-NMR data of **2b** with the related dimethyl and methyl–germyl complexes [18]. Reflecting the high *trans* influence of the $SiPh_3$ ligand, the $^1J_{Pt-P}$ value of P(1) in **2b** is significantly smaller than that of P(2). In contrast, the two phosphorus nuclei in the methyl–germyl complex exhibit almost the same $^1J_{Pt-P}$ values to each other, indicating the comparable *trans* influence of the $GePh_3$ and Me ligands. This observation was supported by X-ray structural analysis.

Silyl ligands exhibit extremely high *trans* effect as well. Representative examples are seen in the ligand exchange reactions of **2a** and **2b** with tertiary phosphines (Scheme 3). Treatment of **2a** with an equimolar amount of PMe_2Ph resulted in selective displacement of $PMePh_2$ *trans* to the $SiPh_3$ ligand [17,25]. The reaction

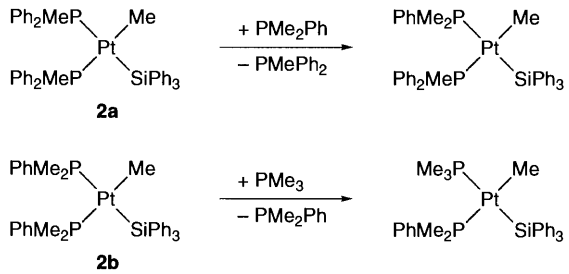

Scheme 3.

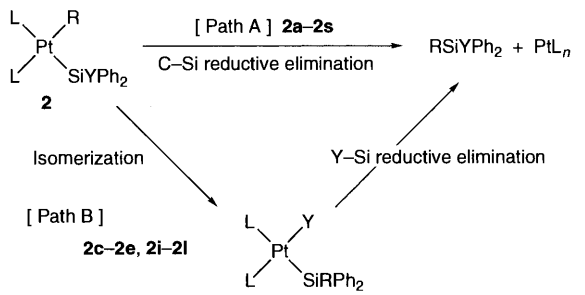

Scheme 4.

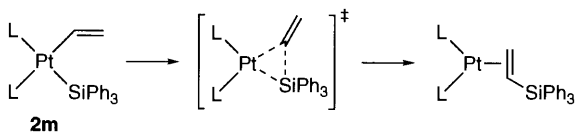

Scheme 5.

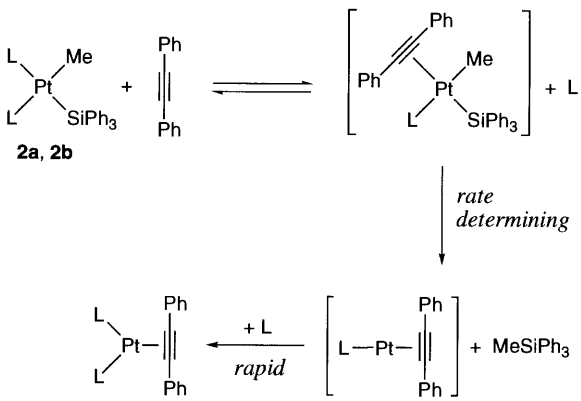

Scheme 6.

of **2b** with PMe_3 also proceeded site-selectively [18]. These reactions were instantly completed at -20°C.

2.2. Mechanisms of C–Si bond formation

Among the organo(silyl)platinum complexes listed in Chart 1, the *trans* isomers **3** were thermally stable. On the other hand, the *cis* isomers **2** underwent C–Si bond formation under appropriate conditions to give the corresponding organosilanes ($RSiYPh_2$) in quantitative yields. Detailed analysis of the thermolysis reactions revealed that the C–Si bond formation proceeds via two reaction pathways, as depicted in Scheme 4. Path A is direct C–Si reductive elimination, whereas Path B is an indirect reaction pathway, comprised of isomerization and reductive elimination processes. Most of the complexes followed Path A, while alkyl complexes bearing a $SiPh_3$ or $SiHPh_2$ ligand, except for methyl–triphenylsilyl complexes **2a** and **2b**, also underwent Path B.

2.2.1. C–Si bond formation via Path A

Vinyl complex **2m** rapidly decomposed at around room temperature in toluene-d_8 to give a platinum(0) complex coordinated with vinylsilane ($k = 1.2 \times 10^{-3}$ s^{-1} at 25.0°C) (Scheme 5) [21]. The reaction rate was not affected by free PMe_2Ph added to the system, indicating a reductive elimination process without dissociation of the phosphine ligand. Complex **2n** having a phenylethenyl ligand exhibited similar kinetic behavior ($k = 2.8 \times 10^{-4}$ s^{-1} at 35.0°C in benzene-d_6) [22].

While alkyl complexes **2a**, **2b**, and **2f**–**h** also gave the corresponding alkylsilanes only by Path A in solution, they showed significantly different thermolysis behavior from **2m** and **2n** [17]. Thus the reaction progress was strongly retarded by addition of free phosphine to the system. The reaction was very slow or not operative in pure solvents, but took place in the presence of an excess amount of alkene or alkyne. Dimethyl acetylenedicarboxylate and maleic anhydride bearing electron-withdrawing substituents served as particularly effective promoters. Diphenylacetylene and styrene also induced the reductive elimination to a considerable extent. On the other hand, the reactions conducted in the presence of simple alkenes such as 1-hexene and 1-octene were slow.

The C–Si reductive elimination from **2a** and **2b** was examined by kinetic experiments in the presence of diphenylacetylene, and the mechanism in Scheme 6 emerged [17,18]. The first step is ligand displacement of one of the phosphine ligands (L) with diphenylacetylene. Taking the much greater *trans* effect of the $SiPh_3$ ligand than the Me ligand into consideration, this step was assumed to take place selectively at the site *trans* to the $SiPh_3$ ligand. The acetylene-coordinated complex thus produced undergoes rate-determining elimination of $MeSiPh_3$.

2.2.2. C–Si bond formation via Path B

Although the methyl–triphenylsilyl complexes **2a** and **2b** smoothly decomposed by Path A at around room temperature in the presence of diphenylacetylene, the ethyl, propyl, and butyl analogs **2c**–**e** having the same $SiPh_3$ ligand were thermally more stable, and mainly

decomposed by the alternative pathway, Path B in Scheme 4. Thus, **2c**–**e** initially isomerized to the corresponding *cis*-PtPh(SiRPh$_2$)L$_2$ complexes (**2q**–**s**), and then afforded alkylsilane by C–Si reductive elimination [19,20].

Fig. 3 shows the change of platinum complexes with time in the thermolysis solution of **2c**, which was followed by NMR spectroscopy at 50°C [20]. It is seen that at the initial stage phenyl(ethyldiphenylsilyl) complex **2q** and Pt(PhC≡CPh)L$_2$ as the reductive elimination product formed simultaneously at the expense of **2c**. The amount of **2q** reached a maximum after approximately 60 min and then gradually decreased, while the amount of Pt(PhC≡CPh)L$_2$ increased further. Finally, **2c** and **2q** disappeared and only the signal of Pt(PhC≡CPh)L$_2$ was observed in the ^{31}P-NMR spectrum. The time-course thus observed was to be in good agreement with the theoretical curves, estimated for concurrent operation of Path A and Path B in Scheme 3. The rates of the isomerization of **2c** to **2q** ($k = 8.0 \times 10^{-5}$ s^{-1}) and the subsequent reductive elimination from **2q** ($k = 2.1 \times 10^{-4}$ s^{-1}) were 1.3 and 3.5 times faster than that of the direct reductive elimination from **2c** ($k = 6.0 \times 10^{-5}$ s^{-1}), respectively.

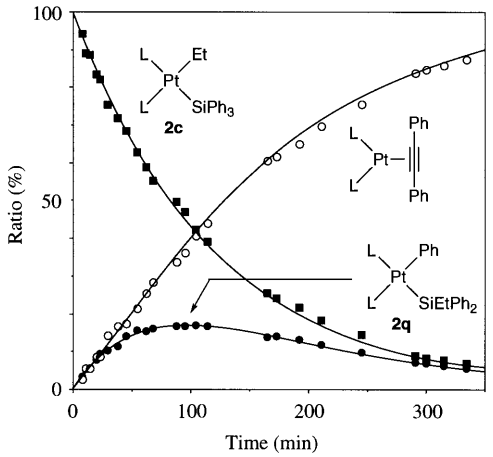

Fig. 3. Time-course of the thermolysis of **2b** in benzene-d_6 at 50°C in the presence of diphenylacetylene: [**2b**]$_0$ = 20 mM, [PhC≡CPh]$_0$ = 0.20 M. The solid lines exhibit calculated reaction curves for concurrent operation of Path A and Path B in Scheme 4.

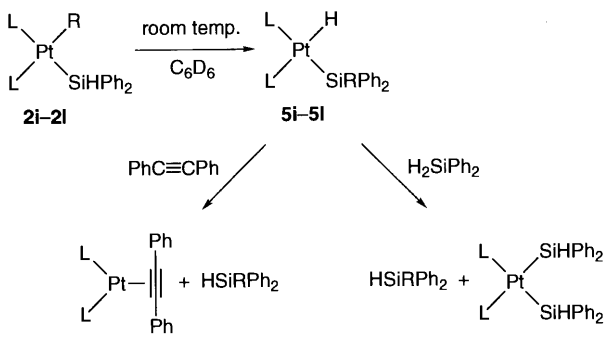

Scheme 7.

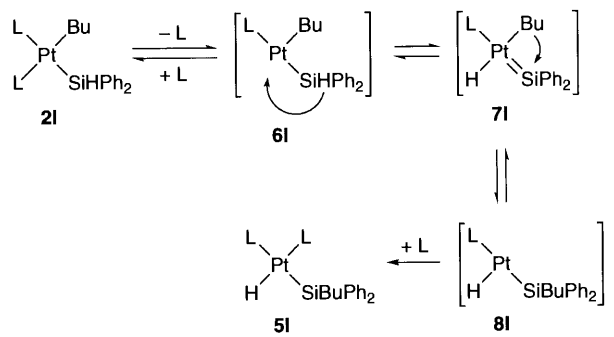

Scheme 8.

Path B was more remarkable for the thermolysis of **2i**–**l** having a SiHPh$_2$ ligand [19]. These complexes, dissolved in benzene-d_6 at room temperature, were converted within a few minutes into the corresponding platinum hydrides *cis*-PtH(SiRPh$_2$)L$_2$ (**5i**–**l**) (Scheme 7). Addition of diphenylacetylene or diphenylsilane to the resulting solutions led to instant liberation of HSiRPh$_2$ in quantitative yields. Hence the C–Si bond formation without C–Si reductive elimination was observed.

Kinetic data suggested the mechanism in Scheme 8 for the isomerization of **2l** to **5l**. The first step is dissociation of PMe$_2$Ph from the site *cis* to the SiHPh$_2$ ligand. The three-coordinate species **6l** thus formed isomerizes to a hydrido–butyldiphenylsilyl complex **8l**, probably via a hydrido–butyl–silylene intermediate **7l**. Coordination of PMe$_2$Ph to **8l** completes the isomerization. The formation of a platinum silylene complex via α-hydrogen elimination from a SiHAr$_2$ ligand has been reported [31]. The C–Si bond formation via migration of an alkyl ligand to a silylene ligand also has a precedent [32].

2.2.3. Comparison of C–Si reductive elimination rates

Table 2 summarizes the rates of C–Si reductive elimination for a series of *cis*-PtR(SiYPh$_2$)(PMe$_2$Ph)$_2$ complexes. The first-order rate constants for **2m** and **2n** were observed in pure solvents without additives. On the other hand, since the reductive elimination from the other complexes required the presence of promoters, the reaction rates were measured under pseudo-first-order kinetics conditions containing an excess amount of diphenylacetylene. While the reactions of **2c**, **2d**, and **2e** proceeded via dual pathways (Scheme 3), only the values for Path A are included in the table.

It is seen that the effects of SiYPh$_2$ groups are modest (entries 7–9 and 10–14), whereas the R groups affect the reaction rates remarkably (entries 1–6 and 14). The reactivity order observed for a series of alkyl–triphenylsilyl complexes (**2b**–**e**: R = Me ≫ Et > Pr ≥ Bu) is of particular interest, because this order is just

Table 2
The first order or pseudo-first-order rate constants for C–Si reductive elimination from *cis*-PtR($SiYPh_2$)(PMe_2Ph)$_2$ complexes (Path A in Scheme 3) [a,b]

Entry	Complex			Additive	Temperature (°C)	10^4 k (s^{-1})
	R	$SiYPH_2$				
1	C=CH_2	$SiPh_3$	**2m**		25.0	12
2	C≡CPh	$SiPh_3$	**2n**		35.0	2.8
3	Me	$SiPh_3$	**2b**	PhC≡CPh (0.20 M)	55.0 (30.0	33 2.2)
4	Et	$SiPh_3$	**2c**	PhC≡CPh (0.20 M)	55.0	1.0
5	Pr	$SiPh_3$	**2d**	PhC≡CPh (0.20 M)	55.0	0.61
6	Bu	$SiPh_3$	**2e**	PhC≡CPh (0.20 M)	55.0	0.58
7	Bu	$SiMePh_2$	**2f**	PhC≡CPh (0.40 M)	40.0	6.9
8	Bu	$SiFPh_2$	**2g**	PhC≡CPh (0.40 M)	40.0	3.7
9	Bu	$Si(OMe)Ph_2$	**2h**	PhC≡CPh (0.40 M)	40.0	2.7
10	Ph	$SiMePh_2$	**2p**	PhC≡CPh (0.20 M)	55.0	4.3
11	Ph	$SiEtPh_2$	**2q**	PhC≡CPh (0.20 M)	55.0	3.5
12	Ph	$SiPrPh_2$	**2r**	PhC≡CPh (0.20 M)	55.0	1.8
13	Ph	$SiBuPh_2$	**2s**	PhC≡CPh (0.20 M)	55.0	1.4
14	Ph	$SiPh_3$	**2o**	PhC≡CPh (0.20 M)	55.0	1.6

[a] The rate constants were measured in benzene-d_6, except for runs 1 and 3 (toluene-d_8).
[b] Initial concentration of **2**: 15–25 mM.

the reverse of the conventional C–C reductive elimination [28,33]. This fact could be rationalized by considering a product-like transition state, in which the R–$SiYPh_2$ bond is nearly formed. The activation barrier mainly reflects the bond energy between the alkyl and silyl groups, which decreases in the order Si–Me ≫ Si–Et > Si–Pr ≥ Si–Bu.

2.2.4. C–Si bond formation in the presence of hydrosilanes

The ethyl, propyl, butyl, and vinyl complexes (**2c**–**2m**) are models of catalytic intermediates for platinum-catalyzed hydrosilylation of alkenes and alkynes. Thus the C–Si reductive elimination from these complexes are generally assumed as the product-forming step of the catalysis [11]. Actually, the vinyl complex **2m** exhibited high reactivity toward C–Si reductive elimination even at room temperature (entry 1 in Table 2). The alkyl complexes bearing $SiHPh_2$ ligand also underwent C–Si bond formation at room temperature according to the process depicted in Scheme 8. However, the other complexes **2c**–**h** were poorly reactive. Thus, although **2c**–**h** afforded alkylsilanes under heated conditions in the presence of diphenylacetylene, the C–Si reductive elimination was extremely slow in the presence of common alkene substrates such as 1-hexene and 1-octene. Therefore, we next examined if the alkylsilane formation takes place in the presence of hydrosilanes, the other substrates of catalytic hydrosilylation [23].

The results are summarized in Scheme 9. The butyl–silyl complexes, except for **2h** (Y = OMe), provided the corresponding butylsilanes in almost quantitative yields (> 97%), together with hydrido(silyl)platinum complexes. The reaction of **2g** was first-order in the concentration of hydrosilane ($k_{obsd} = k$[$HSiFPh_2$][**2**]), showing the selective formation of $BuSiFPh_2$ by the interaction of **2g** with $HSiFPh_2$.

There are two possible mechanisms for the reactions of alkyl(silyl)platinum complexes with hydrosilanes (Scheme 10). One is σ-bond metathesis involving a four-center transition state (Mechanism I), and the other is a sequence of oxidative addition and reductive elimination involving a Pt(IV) species (Mechanism II). While the former mechanism has been well documented for early transition metals complexes having a d^0 metal center [34], its experimental evidence for late transition metal systems is extremely limited [35]. On the other hand, the latter process is commonly assumed for late transition metal-catalyzed reactions. Furthermore, the occurrence of well-defined platinum(IV) complexes by

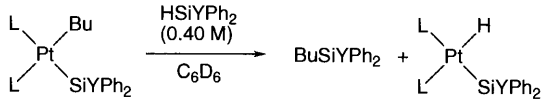

2e–2h

Y	Temp. (°C)	Yield (%)[a]	10^4k (s^{-1})
Ph	55.0	99	1.7
Me	40.0	97	2.7
F	40.0	99	1.6
OMe	60.0	trace	slow

[a] GLC yield.

Scheme 9.

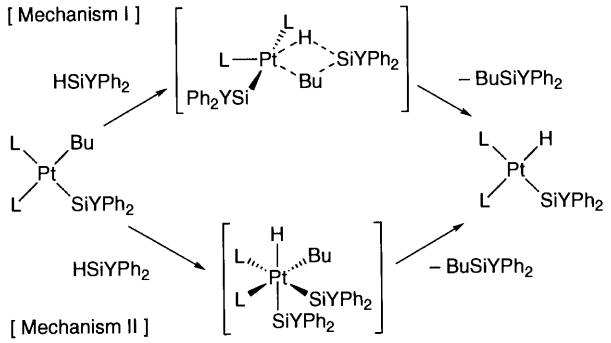

Scheme 10.

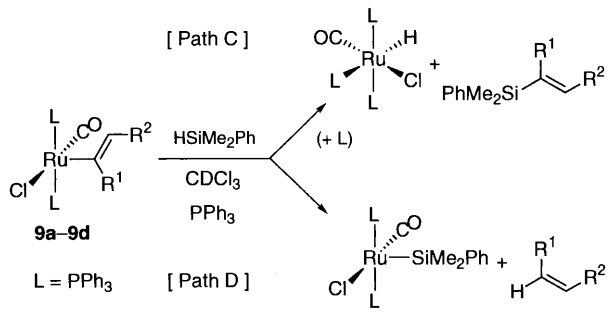

Complex	R^1	R^2	Path C / Path D
9a	H	Ph	99/1
9b	H	*t*-Bu	91/9
9c	Ph	Ph	0/100
9d	CH=CH($SiMe_3$)	$SiMe_2Ph$	0/100

At room temperature. **9**/$HSiMe_2Ph$/PPh_3 = 1/20/1.

Scheme 11.

oxidative addition of hydrosilanes has been recently reported [36]. Nevertheless, an important problem associated with mechanism II still remains unclarified. Thus, to the best of our knowledge, there is no definitive example for the selective C–Si bond formation from an isolated alkyl(hydrido)(silyl)metal species. On the contrary, preferential C–H reductive elimination from such species has been documented [37].

We recently found an interesting dichotomy between the mechanisms of C–Si and C–H bond formation in this connection [38,39]. As shown in Scheme 11, the reactions of alkenylruthenium complexes (**9a**–**d**) with $HSiMe_2Ph$ proceed by either the C–Si or C–H bond formation process (Path C and Path D, respectively). The course-selectivity alters dramatically with the substituents on the alkenyl ligands, particularly with the α-substituent. Thus Path C is mainly operative when the α-substituent is absent (**9a** and **9b**), while Path D proceeds exclusively for the alkenyl complexes bearing an α-substituent (**9c** and **9d**).

Kinetic studies for a series of *para*-substituted styryl complex derivatives strongly suggested the C–Si bond formation mechanism given in Scheme 12 [40]. The first step is a direct association of $HSiMe_2Ph$ with the styryl complexes. The approach of hydrosilane toward ruthenium will take place initially from the compact and electron-rich hydrogen atom. The electrophilic nature of silicon is enhanced by this coordination, leading to nucleophilic attack of the α-carbon of styryl ligand on silicon. The four-center transition state **10** thus produced gives rise to the selective formation of Ru–H and Si–C bonds. The reaction rates exhibited a clear Hammett correlation with σ_p^+ values of the substituents Y ($\rho = -1.07(4)$); the values are known to reflect stabilization of an α-cationic center generated at the *para* position of the substituent in the transition state, as depicted by the limiting structures **10A** and **10B**.

On the other hand, the C–H bond formation for **9d** was found to proceed by oxidative addition of $HSiMe_2Ph$, followed by C–H reductive elimination from a Ru(IV) intermediate.

3. Insertion into a Pt–Si bond

3.1. Effect of cis and trans geometries

Reactivities of *cis*- and *trans*-$PdMe(SiPh_3)L_2$ complexes (**2a**, **2b**, **3a**, and **3b**) were compared for the insertion of phenylacetylene [24,25]. Interestingly, only the *cis* isomers underwent the insertion; the *trans* isomer was totally unreactive or slowly converted to a phenylethynyl complex *trans*-$Pt(C{\equiv}CPh)(SiPh_3)L_2$. This

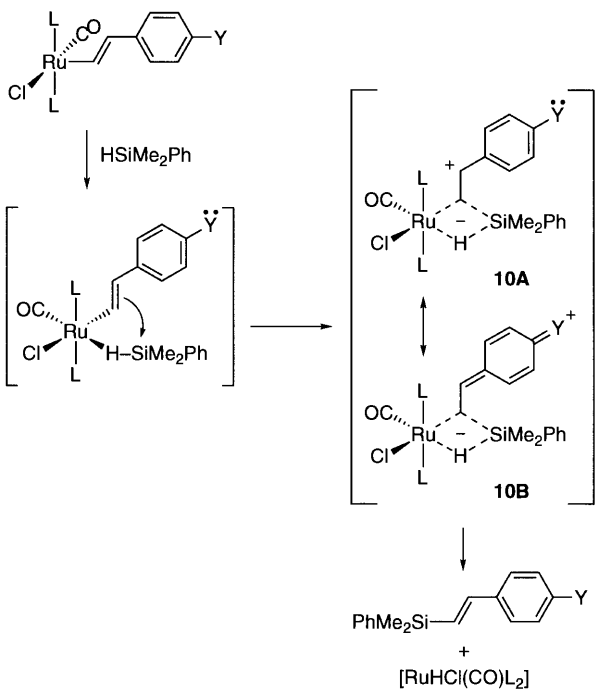

Scheme 12.

striking dependence of the reactivity upon the configuration around platinum was attributable to the ease of ligand displacement of phosphine by phenylacetylene. The occurrence of ligand exchange prior to the insertion was confirmed for a related *cis*-$Pt(COEt)(SiPh_3)(PMe_2Ph)_2$ complex by kinetic investigations.

Scheme 13 illustrates details of the reactions of *cis* isomers. The phenylacetylene insertion competes with the C–Si reductive elimination giving $MeSiPh_3$. Complex **2b** bearing PMe_2Ph ligands gives the insertion complex **12b** in 70% selectivity. On the other hand, the $PMePh_2$ complex **2a** mainly undergoes the C–Si reductive elimination. We proposed that the insertion proceeds via ligand exchange between phenylacetylene and L *trans* to the Me ligand, whereas the C–Si reductive elimination involves prior displacement of L *trans* to the $SiPh_3$ ligand. Actually, the reductive elimination was effectively suppressed by introducing PMe_3, which possesses a higher coordination ability than $PMePh_2$, into the *trans* position of the $SiPh_3$ ligand, causing selective formation of the insertion complex. This fact further supported the reductive elimination mechanism in Scheme 6.

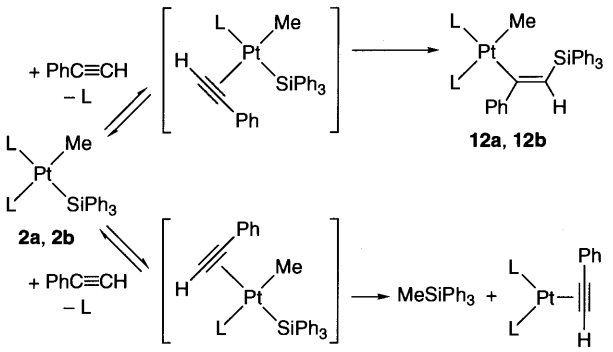

L	Insertion / Reductive elimination
$PMePh_2$ (**2a**)	21/79
PMe_2Ph (**2b**)	70/30

In C_6D_6, at room temperature.

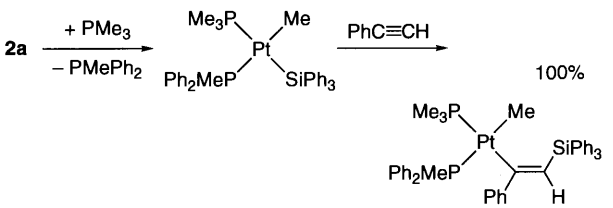

Scheme 13.

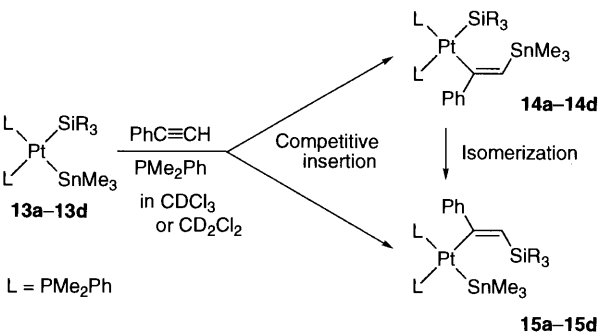

SiR_3	Temp.	Kinetic ratio (**14**/**15**)
$SiMe_3$ (**13a**)	–70 °C	0/100
$SiMe_2Ph$ (**13b**)	–5 °C	34/66
$SiMePh_2$ (**13c**)	15 °C	59/41
$SiPh_3$ (**13d**)	50 °C	93/7

13/PhC≡CH/PMe_2Ph = 1/10/1.

Scheme 14.

3.2. Reactivity of platinum–silyl bonds

We next examined insertion reactions of phenylacetylene into silyl(stannyl)platinum complexes **13a–d** (Scheme 14) [26]. The insertion into the Pt–Sn bond and the Pt–Si bond competed with each other under kinetic conditions. Under thermodynamic conditions, on the other hand, the insertion complexes into the Pt–Si bond (**15a–d**) were exclusively formed. These tendencies are in accordance with the previous theoretical predictions for the alkyne insertion into *cis*-$Pd(SiH_3)(SnH_3)(PH_3)_2$ [41].

The kinetic ratio of **14** to **15** varied significantly with the type of silyl ligand. The $SiMe_3$ complex **13a** gave **14a** exclusively (**14a**/**15a** $\approx$ 0/100), whereas **13d** bearing $SiPh_3$ ligand afforded **15d** predominantly (**14d**/**15d** = 93/7). Complexes **14b** and **14c** exhibited intermediate product ratios (**14b**/**15b** = 34/66; **14c**/**15c** = 59/41). Based on these kinetic ratios, insertion reactivities of the four Pt–SiR_3 bonds relative to the Pt–$SnMe_3$ bond are estimated: $SiMe_3$ (> 49) > $SiMe_2Ph$ (1.9) > $SiMePh_2$ (0.69) > $SiPh_3$ (0.075). This order appears to reflect increasing strength of the Pt–SiR_3 bonds; namely, the M–Si bond dissociation energy is known to increase with increasing electron affinity of silyl ligand, which is enhanced by electron-withdrawing substituents on silicon [15]. A similar tendency was noted for the insertion reaction of unsymmetrical bis-silyl complex *cis*-$Pt(SiMe_2Ph)(SiPh_3)(PMe_2Ph)_2$ with phenylacetylene [27]. In this case, the insertion into the Pt–$SiMe_2Ph$ bond took place in over 96% selectivity.

3.3. Factors governing the reactivity of bis(silyl)platinum complexes

We could evaluate the reactivity order of four Pt–SiR_3 bonds. However, this order was not simply correlated with the insertion reactivities of symmetrical bis-silyl complexes having these Pt–SiR_3 bonds [27].

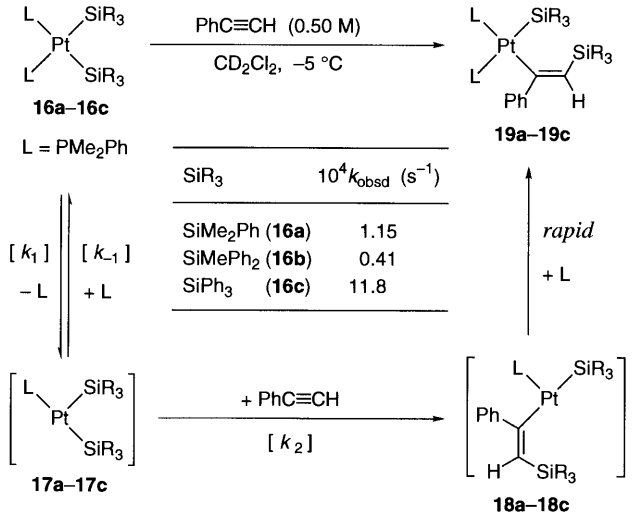

Scheme 15.

Table 3
The rate constants in Scheme 15 for **16a**–**c** [a]

16a (at −5°C)	$k_1 = 1.46(3) \times 10^{-4}$ s^{-1}	$k_2/k_{-1} = 1.35(9) \times 10^{-2}$
16b (at 10°C)	$k_1 = 1.8(1) \times 10^{-3}$ s^{-1}	$k_2/k_{-1} = 1.48(9) \times 10^{-3}$
16c (at −5°C)	$k_1 = 2.8(11) \times 10^{-3}$ s^{-1}	$k_2/k_{-1} = 4.1(13) \times 10^{-4}$

[a] The values were estimated from the $1/k_{obsd} - 1/[PhC{\equiv}CH]$ plots, examined in CD_2CL_2 in the presence of added PMe_2Ph (2.5 mM).

The results are given in Scheme 15. As judging from the pseudo-first-order rate constants (k_{obsd}), which were measured in CD_2Cl_2 at −5°C in the presence of an excess amount of phenylacetylene (0.50 M), the reactivity of three bis-silyl complexes decreases in the order **16c** > **16a** > **16b**, which is apparently inconsistent with the reactivity order observed for the Pt–SiR_3 bonds under kinetic conditions. The most significant is the highest insertion rate of **16c**, which has the least reactive Pt–$SiPh_3$ bonds.

The reason for this disagreement could be gained from kinetic data. As depicted in Scheme 15, the phenylacetylene insertion into bis-silyl complexes involves prior dissociation of one of the PMe_2Ph ligands, giving a three-coordinate intermediate **17**, which successively undergoes insertion of phenylacetylene into the Pt–Si bond. The resulting alkenyl–silyl complex **18** is then rapidly converted to the final product **19** by *trans* to *cis* isomerization followed by coordination of PMe_2Ph liberated in the system.

Table 3 lists the rate constants for each elementary step (i.e. k_1 and k_2/k_{-1} in Scheme 15). It is seen that the k_2/k_{-1} value for **16a** is 33 times larger than that for **16c**. This fact is consistent with the higher reactivity of Pt–$SiMe_2Ph$ bond than Pt–$SiPh_3$ bond toward insertion (vide infra). Even in this situation, however, **16c** reacts more rapidly with phenylacetylene than **16a**. This is because **16c** undergoes the dissociation of PMe_2Ph more readily than **16a** (see the k_1 values in Table 3). The k_1 value of **16b** with the least reactivity is 1.8×10^{-3} s^{-1} at 10°C, which corresponds to the approximate value of 0.9×10^{-4} s^{-1} at −5°C on the basis of activation parameters. Accordingly, it is concluded that the reactivities of **16a**–**c** are mainly controlled by the rates of dissociation of PMe_2Ph.

Fig. 4 shows the X-ray structures of **16a** − **c**, together with the $^{31}P\{^1H\}$-NMR data. As already pointed out for **16b** by Tsuji et al. [42], the bis(silyl)platinum complexes have a twisted square planar geometry around platinum, distinctly distorted from planarity in the order **16a** < **16c** < **16b**. Since the theoretical structure of *cis*-$Pt(SiH_3)_2(PH_3)_2$ has no such distortion [43], the structural variation observed for **16a**–**c** may be attributed primary to the difference in bulkiness of silyl ligands. Actually, the distances between the two silicon

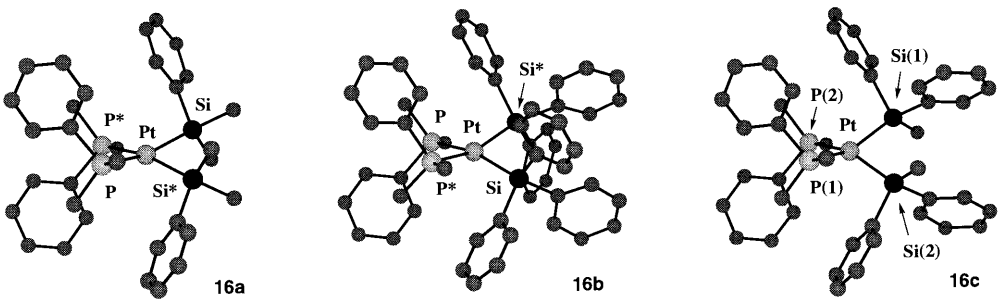

		16a	16b	16c
Pt–Si	(Å):	2.370(1)	2.358(1)	2.374(3), 2.373(3)
Pt–P	(Å):	2.370(0)	2.354(1)	2.396(2), 2.408(3)
Si ··· Si	(Å);	3.233(1)	3.303(2)	3.334(4)
Si–Pt–Si	(deg):	86.02(5)	88.93(5)	89.22(9)
P–Pt–P	(deg):	93.63(5)	96.72(6)	93.49(9)
DA	(deg):	22.8	38.7	28.3
$^1J_{Pt-P}$	(Hz):	1528	1560	1508

Fig. 4. CHEM-3D views of the X-ray structures of bis(silyl)platinum complexes **16a** ($R = 0.026$), **16b** ($R = 0.044$), and **16c** ($R = 0.042$).

atoms (Si–Si) and the Si–Pt–Si angles are significantly larger than the calculated ones (3.111 Å and 82.0°) and increase with increasing bulkiness of silyl ligands (**16a** < **16b** < **16c**). On the other hand, dihedral angles between the PtP_2 and the $PtSi_2$ plane exhibit irregularity in their order (**16a** < **16c** < **16b**), not simply accounted for by steric congestion around platinum. Thus **16b** with medium sized $SiMePh_2$ ligands has the most twisted structure, while **16c** with the biggest $SiPh_3$ ligands shows the medium dihedral angle. It is further noted that **16b**, with the most twisted structure, has the shortest Pt–Si and Pt–P bonds. Since bond lengths between the metal center and coordinated atoms in square planar complexes are known to vary with *trans* influence, the significant distortion in **16b**, which reduces the direct labilizing interaction between mutually *trans* ligands, may be responsible for the shortest bonds. It is also seen that the Pt–P bond lengths determined by X-ray structural analysis are nicely correlated with the $^1J_{Pt-P}$ values observed in $^{31}P\{^1H\}$NMR spectra. Thus the Pt–P distances in the crystals decrease as the $^1J_{Pt-P}$ constants increase. Therefore, we may consider that the structural features observed in the crystals are preserved in solution as well.

Similarly to *cis*-MR_2L_2 complexes of Group 10 metals (R = alkyl, L = tertiary phosphine) [33a], the silyl ligands in **16a**–**c** combine with the $Pt(PMe_2Ph)_2$ moiety *via* two types of bonding orbitals given in Chart 2. The a_1 and b_2 symmetry orbitals in this scheme are roughly assigned to donation ($\sigma \rightarrow$ d) and back-donation (d $\rightarrow \sigma^*$) interactions between the combination of two SiR_3 ligands and the platinum center, respectively. Unlike the dialkyl complexes, the present complexes have silyl ligands, which are much more electron-releasing than alkyl ligands. Therefore, the a_1 type orbital interaction can predominate over the b_2 type interaction. In this situation, bis-silyl complex has a significantly distorted structure when the distortion is needed to relieve the steric repulsion between the ligands. The higher distortion in **16b** than **16a** can be rationalized in this context; namely, the sterically more demanding $SiMePh_2$ ligand leads to the more twisted structure, and the steric strain inherent in **16b** is effectively relieved by this distortion. In addition, the distortion also reduces direct *trans* influence of the silyl ligands on the Pt–P bonds. Indeed, **16b** has the shortest Pt–P bonds and the largest $^1J_{Pt-P}$ constant. These situations give rise to the stability of **16b** toward the dissociation of PMe_2Ph and reduce the insertion rate.

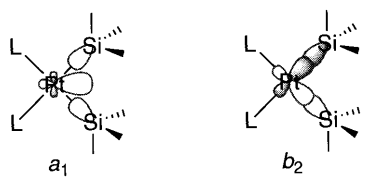

Chart 2.

On the other hand, when the silyl ligand has electron-withdrawing (or less electron-releasing) substituents and possesses an electron-withdrawing character, the b_1 type orbital interaction gains importance, compelling the planarity of bis(silyl) complex. Complex **16c** should be the case, in which the distortion is modest despite the presence of the most sterically demanding $SiPh_3$ ligands. This situation must provide significant strain energy for **16c**, which will be efficiently released by dissociation of one of the PMe_2Ph ligands. Furthermore, the more planar structure causes the more effective weakening of the Pt–P bonds by silyl ligands with great *trans* influence; **16c** actually has the longest Pt–P bonds and the smallest $^1J_{Pt-P}$ constant (Fig. 4). Consequently, **16c** is highly reactive to the dissociation of PMe_2Ph and hence to the insertion of phenylacetylene.

4. Conclusion

Although the mechanisms of catalytic addition of silicon–element bonds to carbon–carbon multiple bonds are frequently discussed by an extension of conventional organometallic chemistry, the present study has clearly indicated that the silyl metal intermediates are significantly unique in their structures and reactivities. The use of kinetic techniques in combination with well-defined complexes is a powerful means of gaining a deep understanding of such chemistry.

Acknowledgements

I would like to thank my active co-workers, whose names are listed in the references. This work was supported by a Grant-in-Aid for Scientific Research on Priority Area The Chemistry of Inter-element Linkage (No. 09239105) from the Ministry of Education, Science, Sports and Culture, Japan.

References

[1] I. Beletskaya, C. Moberg, Chem. Rev. 99 (1999) 3435.
[2] F. Ozawa, Syokubai Catal. Catal. 41 (1999) 199.
[3] (a) B. Marciniec, Comprehensive Handbook of Hydrosilylation, Pergamon Press, Oxford, 1992. (b) T. Hiyama, T. Kusumoto, Comprehensive Organic Synthesis, vol. 8, in: B.M. Trost, I. Fleming (Eds.), Pergamon Press, Oxford, 1991, p. 763. (c) I. Ojima, The Chemistry of Organic Silicon Compounds, in: S. Patai, Z. Rappoport (Eds.), Wiley, Chichester, 1989, p. 1479.
[4] (a) K.A. Horn, Chem. Rev. 98 (1995) 1317. (b) H.K. Sharma, K.H. Pannell, Chem. Rev. 95 (1995) 1351.
[5] (a) M. Suginome, H. Nakamura, Y. Ito, Chem. Commun. (1996) 2777. (b) S. Onozawa, Y. Hatanaka, M. Tanaka, Chem. Commun. (1997) 1229. (c) M. Suginome, H. Nakamura, Y. Ito, Angew. Chem. Int. Ed. Engl. 36 (1997) 2516. (d) M. Suginome,

H. Nakamura, T. Matsuda, Y. Ito, J. Am. Chem. Soc. 120 (1998) 4248. (e) M. Suginome, T. Matsuda, H. Nakamura, Y. Ito, Tetrahedron 55 (1999) 8787.
[6] For related studies using borylstannanes, see: (a) S. Onozawa, Y. Hatanaka, T. Sakakura, S. Shimada, M. Tanaka, Organometallics 15 (1996) 5450. (b) S. Onozawa, Y. Hatanaka, N. Choi, M. Tanaka, Organometallics 16 (1997) 5389. (c) S. Onozawa, Y. Hatanaka, M. Tanaka, Tetrahedron Lett. 39 (1998) 9043. (d) S. Onozawa, Y. Hatanaka, M. Tanaka, Chem. Commun. (1999) 1863.
[7] (a) T.N. Mitchell, H. Killing, R. Dicke, R. Wickenkamp, J. Chem. Soc. Chem. Commun. (1985) 354. (b) B.L. Chenard, E.D. Lagnis, F. Davidson, T.V. RajanBabu, J. Org. Chem. 50 (1985) 3666. (c) B.L. Chenard, C.M. Van Zyl, J. Org. Chem. 51 (1986) 3561 (d) T.N. Mitchell, R. Wickenkamp, A. Amamria, R. Dicke, U. Schneider, J. Org. Chem. 52 (1987) 4868. (e) M. Murakami, Y. Morita, Y. Ito, J. Chem. Soc. Chem. Commun. (1990) 428. (f) Y. Tsuji, Y. Obora, J. Am. Chem. Soc. 113 (1991) 9368. (g) Y. Obora, Y. Tsuji, M. Asayama, T. Kawamura, Organometallics 12 (1993) 4697. (h) Y. Obora, Y. Tsuji, T. Kawamura, J. Am. Chem. Soc. 117 (1995) 9814. (i) Y. Obora, Y. Tsuji, T. Kakehi, M. Kobayashi, Y. Shinkai, M. Ebihara, T. Kawamura, J. Chem. Soc. Perkin Trans. 1 (1995) 599.
[8] L.B. Han, M. Tanaka, J. Am. Chem. Soc. 120 (1998) 8249.
[9] N. Auner, From Molecules to Materials, in: J. Weis (Ed.), Organosilicon Chemistry I–IV, VCH, Weinheim, 1994, 1996, 1997, 2000.
[10] J.Y. Corey, J. Braddock-Wilking, Chem. Rev. 99 (1999) 175.
[11] (a) P. Braunstein, M. Knorr, J. Organomet. Chem. 500 (1995) 21. (b) T.D. Tilley, The Chemistry of Organic Silicon Compounds, in: S. Patai, Z. Rappoport (Eds.), Wiley, Chichester, 1989, p. 1415.
[12] (a) Y. Kiso, K. Tamao, M. Kumada, J. Organomet. Chem. 76 (1974) 105. (b) C. Eaborn, T.N. Metham, A. Pidcock, J. Organomet. Chem. 131 (1977) 377. (c) D. Seyferth, E.W. Goldman, J. Escudié, J. Organomet. Chem. 271 (1984) 337. (d) T. Kobayashi, T. Hayashi, H. Yamashita, M. Tanaka, Chem. Lett. (1989) 467. (e) M. Tanaka, Y. Uchimaru, H. Lautenschlager, J. Organomet. 10 (1991) 16. (f) Y. Pan, J.T. Mague, M. Fink, J. Organomet. 11 (1992) 3495. (g) M. Murakami, T. Yoshida, Y. Ito, Organometallics 13 (1994) 2900. (h) F. Ozawa, M. Sugawara, T. Hayashi, Organometallics 13 (1994) 3237. (i) M. Suginome, H. Oike, S.S. Park, Y. Ito, Bull. Chem. Soc. Jpn. 69 (1996) 289. (j) M. Suginome, Y. Ito, J. Chem. Soc. Dalton Trans. (1998) 1925. (k) M. Murakami, T. Yoshida, S. Kawanami, Y. Ito, J. Am. Chem. Soc. 117 (1995) 6408.
[13] (a) J. Chatt, C. Eaborn, P.N. Kapoor, J. Organomet. Chem. 23 (1970) 109. (b) H. Yamashita, M. Tanaka, M. Goto, Organometallics 12 (1993) 988.
[14] Y. Tanaka, H. Yamashita, S. Shimada, M. Tanaka, Organometallics 16 (1997) 3246.
[15] For theoretical studies, see the account reported by Sakaki in this issue, see also: S. Sakaki, N. Mizoe, M. Sugimoto, Y. Musashi, Coord. Chem. Rev. 190 (1999) 933.
[16] (a) C.J. Levy, R.J. Puddephatt, J. Am. Chem. Soc. 119 (1997) 10127. (b) B. Biswas, M. Sugimoto, S. Sakaki, Organometallics 18 (1999) 4015.
[17] F. Ozawa, T. Hikida, T. Hayashi, J. Am. Chem. Soc. 116 (1994) 2844.
[18] F. Ozawa, T. Hikida, K. Hasebe, T. Mori, Organometallics 17 (1998) 1018.
[19] F. Ozawa, M. Kitaguchi, H. Katayama, Chem. Lett. (1999) 1289.
[20] K. Hasebe, J. Kamite, T. Mori, H. Katayama, F. Ozawa, Organometallics 19 (2000) 2022.
[21] F. Ozawa, T. Tani, M. Mori, H. Katayama, unpublished results.
[22] F. Ozawa, M. Mori, unpublished results.
[23] F. Ozawa, M. Kitaguchi, H. Katayama, unpublished results.
[24] T. Hikida, K. Onitsuka, K. Sonogashira, T. Hayashi, F. Ozawa, Chem. Lett. (1995) 985.
[25] F. Ozawa, T. Hikida, Organometallics 15 (1996) 4501.
[26] F. Ozawa, Y. Sakamoto, T. Sagawa, R. Tanaka, H. Katayama, Chem. Lett. (1999) 1307.
[27] F. Ozawa, J. Kamite, Organometallics 17 (1998) 5630.
[28] A. Yamamoto, Organotransition Metal Chemistry: Fundamental Concepts and Applications, Wiley, New York, 1986, p. 240.
[29] (a) F. Ozawa, T. Ito, Y. Nakamura, A. Yamamoto, Bull. Chem. Soc. Jpn. 54 (1981) 1868. (b) H. Nakazawa, F. Ozawa, A. Yamamoto, Organometallics 2 (1983) 241. (c) F. Ozawa, K. Kurihara, M. Fujimori, T. Hidaka, T. Toyoshima, A. Yamamoto, Organometallics 8 (1989) 180.
[30] F. Ozawa, K. Kurihara, T. Yamamoto, A. Yamamoto, J. Organomet. Chem. 279 (1985) 233.
[31] (a) G.P. Mitchell, T.D. Tilley, Angew. Chem. Int. Ed. 37 (1998) 2524. (b) G.P. Mitchell, T.D. Tilley, J. Am. Chem. Soc. 120 (1998) 7635.
[32] M. Okazaki, H. Tobita, H. Ogino, J. Chem. Soc. Dalton Trans. (1997) 3531.
[33] (a) K. Tatsumi, R. Hoffmann, A. Yamamoto, J.K. Stille, Bull. Chem. Soc. 54 (1981) 1857. (b) J.M. Brown, N.A. Cooley, Chem. Rev. 88 (1988) 1031.
[34] (a) B.A. Arndtsen, R.G. Bergman, T.A. Mobley, T.H. Peterson, Acc. Chem. Res. 28 (1995) 154. (b) R.H. Crabtree, Chem. Rev. 95 (1995) 987.
[35] (a) X.L. Luo, R.H. Crabtree, J. Am. Chem. Soc. 111 (1989) 2527. (b) J.F. Hartwig, S. Bhandari, P.R. Rablen, J. Am. Chem. Soc. 116 (1994) 1839. (c) C.N. Iverson, M.R. Smith III, J. Am. Chem. Soc. 117 (1995) 4403. (d) J.C. Lee Jr., E. Peris, A.L. Rheingold, R.H. Crabtree, J. Am. Chem. Soc. 116 (1994) 11014. (e) T.B. Marder, N.C. Norman, C.R. Rice, E.G. Robins, Chem. Commun. (1997) 53.
[36] (a) S. Shimada, M. Tanaka, M. Shiro, Angew. Chem. Int. Ed. Engl. 35 (1996) 1856. (b) S. Shimada, M.L.N. Rao, M. Tanaka, Organometallics 18 (1999) 291, and references cited therein.
[37] (a) M. Aizenberg, D. Milstein, J. Am. Chem. Soc. 117 (1995) 6456. (b) S.B. Duckett, R.N. Pertsz, Organometallics 11 (1992) 90. (c) M.E. van der Boom, J. Ott, D. Milstein, Organometallics 17 (1998) 4263.
[38] Y. Maruyama, K. Yamamura, F. Ozawa, Chem. Lett. (1998) 905.
[39] For related studies, see: (a) Y. Maruyama, K. Yamamura, I. Nakayama, K. Yoshiuchi, F. Ozawa, J. Am. Chem. Soc. 120 (1998) 1421. (b) Y. Maruyama, K. Yoshiuchi, F. Ozawa, Y. Wakatsuki, Chem. Lett. (1997) 623. (c) Y. Maruyama, K. Yoshiuchi, F. Ozawa, J. Organomet. Chem. 609 (2000) 130.
[40] Y. Maruyama, K. Yamamura, T. Sagawa, H. Katayama, F. Ozawa, Organometallics 19 (2000) 1308.
[41] M. Hada, Y. Tanaka, M. Ito, M. Murakami, H. Amii, Y. Ito, H. Nakatsuji, J. Am. Chem. Soc. 116 (1994) 8754.
[42] (a) Y. Tsuji, K. Nishiyama, S. Hori, M. Ebihara, T. Kawamura, Organometallics 17 (1998) 507. (b) Y. Obora, Y. Tsuji, Y. Nishiyama, M. Ebihara, T. Kawamura, J. Am. Chem. Soc. 118 (1996) 10922.
[43] S. Sakaki, M. Ogawa, M. Kinoshita, J. Phys. Chem. 99 (1995) 9933.